An Integral Approach to Free-Form Object Modeling

Heung-Yeung Shum, *Member, IEEE*,
Martial Hebert, *Senior Member, IEEE*,
Katsushi Ikeuchi, *Senior Member, IEEE*,
and Raj Reddy, *Fellow, IEEE*

Abstract—This paper presents a new approach to free-form object modeling from multiple range images. In most conventional approaches, successive views are registered sequentially. In contrast to the sequential approaches, we propose an integral approach which reconstructs statistically optimal object models by simultaneously aggregating all data from multiple views into a weighted least-squares (WLS) formulation. The integral approach has two components. First, a global resampling algorithm constructs partial representations of the object from individual views, so that correspondence can be established among different views. Second, a weighted least-squares algorithm integrates resampled partial representations of multiple views, using the techniques of principal component analysis with missing data (PCAMD). Experiments show that our approach is robust against noise and mismatch.

Index Terms—3D object modeling, free-form object modeling, multiple view merging, principal component analysis, resampling, local curvature.

———————————— ✦ ————————————

1 INTRODUCTION

AS an alternative to building objects manually, observation-based modeling automatically constructs solid models from real objects using computer vision techniques. Applications of observation-based modeling include, among others: creating models for animation, reconstructing human body parts for surgical planning, recovering machine parts for virtual factory simulation, and building CAD models for model-based recognition.

Usually, observation-based modeling systems work with a sequence of images of the object(s), where the sequence spans a smoothly varying change in the positions of the sensor and/or object(s). The task of observation-based modeling is essentially the problem of merging multiple views using an appropriate representation. Many previous observation-based modeling techniques involve motion estimation between successive pairs of views in a sequential manner [10], [13], [19], as shown in Fig. 1a. Whenever a new view is introduced, it is matched with the previous view. The transformation between these two successive views has to be accurately estimated before the object model is updated. However, data acquisition and image registration introduce significant errors. Range images have missing data points due to occlusion and self-occlusion [2]. Thus, transformation errors accumulate and propagate from one matching to another. This sequential method may result in noticeably imprecise object models.

- *H.-Y. Shum is with Microsoft Research, One Microsoft Way, Redmond, WA 98052-6399. E-mail: hshum@microsoft.com.*
- *M. Hebert is with the Robotics Institute, Carnegie Mellon University, 5000 Forbes Ave., Pittsburgh, PA 15213.*
- *K. Ikeuchi is with the Institute of Industrial Science, University of Tokyo, Roppongi, 7-22-1, Minakto-ku, Tokyo, Japan. E-mail: ki@iis.u-tokyo.ac.jp.*
- *R. Reddy is with the School of Computer Science, Carnegie Mellon University, 5000 Forbes Ave., Pittsburgh, PA 15213.*
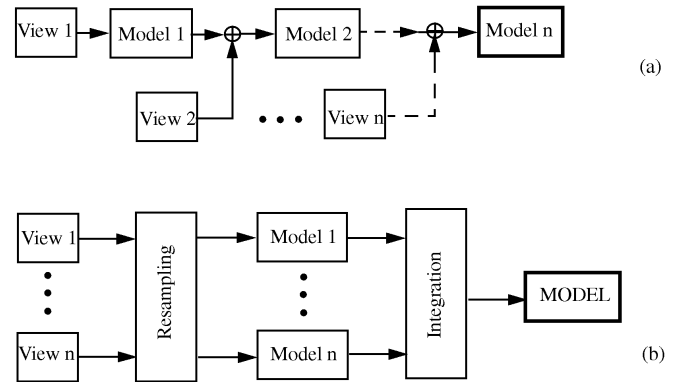
Fig. 1. Observation-based model systems: (a) sequential modeling; (b) integral modeling.

In this paper, we present a new technique for observation-based modeling of free-form objects. This technique, called *integral approach*, is illustrated in Fig. 1b. Rather than sequentially integrating successive pairs of views, we propose to reconstruct a statistically optimal object model that is simultaneously most consistent with all the views. Our method makes use of significant redundancy existing among all the views, i.e., it is likely that any part of the object will be observed a number of times along the sequence of images, although each single view provides only partial information.

In previous work, we have applied the integral approach to polyhedral object modeling, where polyhedral object models and view transformations are recovered simultaneously by employing the principal component analysis with missing data (PCAMD) algorithm [15]. Unlike planar patches in polyhedral object modeling [15], however, correspondence of range images of curved surfaces is a difficult problem. Due to discrete sampling, data points in two different views generally do not correspond with each other. On the other hand, salient features, such as high curvature points, do correspond with each other but are difficult to reliably extract from noisy range data of a single view.

We propose to determine correspondence by resampling each view of the free-form object. In particular, this resampling process combines top-down topological knowledge (a spherical surface representation) with bottom-up geometrical properties (approximated local curvature). For each range image, we first build a discrete mesh that approximates the object's surface and encodes the local curvature at each node. The local curvature at each node is integrated from its neighborhood. During the process of mesh approximation, local connectivity among different nodes is always preserved, i.e., each mesh node has exactly three neighbors. Mesh matching is based on the local curvature distribution at each mesh node. Global resampling is applied on the spherical mesh coordinate system to establish one-to-one correspondence among mesh nodes from multiple views.

The remainder of this paper is organized as follows. After reviewing previous work on modeling from multiple range images in Section 2, we introduce our integral approach to object modeling in Section 3 and Section 4. In Section 3, we address the problem of "what to integrate" by presenting a novel global resampling scheme which can be used to determine correspondence among different views. In Section 4, we show "how to integrate" by solving a two-step weighted least-squares problem from the measurement matrix which is formed by resampling the whole sequence of range images. We demonstrate the robustness of our proposed PCAMD method by applying it to real range images. We close with a discussion of future work, along with a summary.

2 PREVIOUS WORK

Most work on modeling from multiple range images assumed that the transformation between successive views is either known or can be recovered, so that all data can be transformed with respect to a fixed coordinate system. Bhanu [4] modeled an object by rotating it through known angles. Ahuja and Veenstra [1] constructed an octree object model from orthogonal views. By finding the correspondences from intensity patterns in all eight views, Vemuri and Aggarwal [21] derived the motion and transformed all eight range images with respect to the first frame.

To accurately recover the transformation between two views, different range image registration techniques using various features have been proposed. Ferrie and Levine [9] used correspondence points which were identified by correlation over the differential properties of the surface. Parvin and Medioni [13] proposed the construction of boundary representation (B-rep) models using segmented surface patches. The difficulty of feature-based registration is in realizing robustness, especially in the case of free-form objects.

Many algorithms also exist for featureless range data point matching. Besl and Kay [3] used the iterative point matching (ICP) method to project points from one surface to another during matching. A similar approach was proposed by Chen and Medioni [6]. Champleboux et al. [5] used the Levenberg-Marquart nonlinear minimization algorithm to minimize the sampled distance to surface using octree-splines. These featureless registration algorithms are locally optimal; they work well only if a good initial transformation is given.

After transforming all range images to a world coordinate system using the registration result, an object model is usually obtained by running a connectivity algorithm (such as the Delaunay triangulation) at the last step. Hoppe et al. [11] used graph traversal methods. Connectivity can also be modified and determined as more views are incorporated. Parvin and Medioni [13] used an adjacency graph to represent the connectivity of each segmented view. Soucy and Laurendeau [17] made use of the structured information about where the images are taken; they proposed to triangulate each view and merge multiple views via a Venn diagram when the transformation is known. The common parts of different views are then resampled. Turk and Levoy [19] proposed a similar approach, but avoided the problem of Venn diagram construction by merging only two adjacent views at each step.

3 WHAT TO INTEGRATE: GLOBAL RESAMPLING

To integrate multiple views in a statistically optimal fashion, we first need to determine what is to be integrated from a sequence of range data. In our previous work on polyhedral object modeling [15], we have successfully made use of the redundancy in multiple views by tracking planar surface patches over the sequence. Ideally, for free-form object modeling, we would like to register each data point from one view to another. However, the physical correspondences between data points in two different views are usually not known a priori. As a result, we have to search for some salient features which do have correspondence among different views.

Because curvature is invariant under Euclidean group transformations, we would have physical correspondence among distinguished high curvature points in different views. In practice, however, from a particular viewing direction, we obtain only a finite number of sampling points of a surface. These points are measured in the sensor coordinate system. The normals, or the tangent planes, as well as the curvatures, are not explicitly or directly known. Although surface normals can be approximated by fitting local planar surface patches of points, the process of computing curvature at each point using range data is known to be highly noise sensitive and may be numerically unstable.

To address the problem of what to integrate from multiple range images of a known topology object, we propose a global resampling scheme, including spherical surface representation, deformable mesh generation, and one-to-one mesh node correspondence. In this paper, we focus only on objects with spherical topology.

For each range image, we first build a discrete mesh that approximates the object's surface, and encodes the local curvature. Mesh matching is based on the local curvature distribution at each mesh node. Using the spherical mesh coordinate system, global resampling is used to establish one-to-one correspondence among mesh nodes from multiple views.

The concept of global resampling is based on previous work on spherical surface representation and matching for object recognition [8]. We describe only the basic approach of the spherical surface representation and the main result of curvature-based matching, and refer the reader to [8] for a detailed description of the algorithms.

3.1 Surface Representation Using Deformable Mesh

Our basic surface representation is a discrete connected mesh that is homeomorphic to a sphere. The free-form objects are restricted to a topology of genus zero (i.e., no holes) in this paper. A distinctive feature of our surface representation is its global structure, i.e., the connectivity of the mesh is such that each node has exactly three neighbors. The total number of mesh nodes depends on the resolution of the mesh.

Different attributes may be associated with each node of the mesh. An approximation of curvature, called the simplex angle, is computed at each node from its position and the positions of its three neighbors. We use $g(P)$ to denote the simplex angle at node P. The semi-regularly tessellated unit sphere with simplex angle at each mesh node is called a simplex angle image (SAI) [8]. Other methods can also be used to compute curvature at each mesh node. For example, Taubin [18] showed an efficient method to calculate curvatures from nonsmooth surfaces using eigenvalues and eigenvectors of certain 3×3 symmetric matrices.

Given a set of data points from a range image, the mesh representation is constructed by first placing a spherical or ellipsoidal mesh at the approximate center of the object, then iteratively deforming the shape of the mesh in response to "forces" generated by the data points and the image features, as well as by internal smoothness constraints. Many deformable models, such as irregular meshes [20], finite element models [12], and balloon models [7] have been proposed for 3D shape reconstruction.

A surface model reconstruction from a range image is shown in Fig. 2. The mesh is always a closed surface. However, since only part of the object's surface is visible from a given viewpoint, some of the mesh nodes do not correspond to visible surface data. These nodes, corresponding to the occluded part of the object, are flagged as interpolated nodes, so that they can be treated differently when used. We should point out that the deformable surface is more suitable for representing rather smooth objects because it has the tendency to smooth out high curvature regions (or significant internal discontinuity on the object).

3.2 Mesh Matching

In order to compare two meshes, we need to find the correspondence between the two sets of mesh nodes. In general, such a correspondence may not exist because the distributions of nodes on the two surfaces may be completely different. To obviate this problem, we introduce a regularity constraint on the distribution of the nodes on the surface. This constraint can be evaluated locally at each node which has exactly three neighbors and is incorporated in an iterative fitting algorithm as an additional force. When this constraint is enforced, meshes representing the same
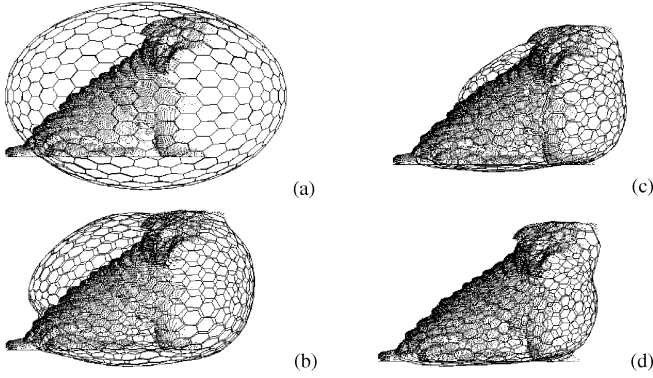
Fig. 2. Deformable surface reconstruction at different iteration steps (dots are range data, solid lines are mesh models) (a) n = 0 (start of deformation); (b) n = 20; (c) n = 50; (d) n = 100 (end of deformation).

surface viewed from different viewpoints have the property that their nodes do correspond.

Given meshes from two views, the matching proceeds by comparing the simplex angles at the nodes of the two meshes. Specifically, if $\{P_i\}$ and $\{Q_j\}$ are the nodes of the two meshes, we search for the correspondence that minimizes the "distance" between two meshes:

$$D(S, S') = \sum_C \left(g(P_i) - g(Q_j) \right)^2, \qquad (1)$$

where $g(P)$ is the simplex angle at a mesh node P, C is the correspondence set between mesh nodes of the two meshes. Since the local curvature is independent of the translation, we can search for the best match only in the rotation space. The connectivity among all mesh nodes can further simplify the mesh matching [10].

Once the best set of correspondences is obtained, we compute an estimate of the transformation (R, T) between the two views by minimizing the distance:

$$\sum_C \left\| P_i - \left(\mathbf{R}Q_j + \mathbf{T} \right) \right\|^2. \qquad (2)$$

The resulting transformation $(\mathbf{R}, \mathbf{T})$ is only an initial estimate because the nodes P_i and Q_j do not correspond exactly due to the resolution of the mesh.

3.3 One-to-One Correspondence

In order to apply the PCAMD algorithm to take advantage of redundancy of multiple views, we need one-to-one mapping among different views. The matching procedure above, however, does not guarantee one-to-one correspondence between two sets of mesh nodes generated from two views because of the discrete sampling and the requirement of local regularity.

We establish the one-to-one correspondence by resampling each deformable surface using the global spherical coordinate. The correspondence between two meshes that approximates two range images is not the correspondence between their mesh nodes, but rather that between their parameterization using the global coordinate. Once a set of spherical mesh nodes (along with its local curvature attributes) is obtained, it is possible to interpolate any point on the spherical coordinate from this set. For example, in Fig. 3, although there exist many-to-one mappings between $\mathbf{P}$ and $\mathbf{Q}$ (both P_1 and P_2 are matched to Q_1), mapping between P' and $\mathbf{P}$ is one-to-one because P' results from the rotation of P. The new mesh node at P'_1 and its simplex angle can be interpolated from its nearest point Q_1 on set $\mathbf{Q}$ and three neighbors of Q_1. Let $g(P')$ and $g(Q_1)$ be the values of the simplex angles at node P' and its nearest node Q_1, respectively. We have the following local interpolation:

$$g(P') = \sum_{i=1}^{4} w_i g(Q_i), \qquad (3)$$

where Q_2, Q_3, and Q_4 are three neighbors of Q_1, and w_i are the weights depending on the distance between P' and Q_i ($i = 1, 2, 3, 4$). The coordinates of the mesh node at P' can be interpolated in the same way. Because of the one-to-one mapping between any two views, one-to-one mapping among multiple views can be established. When the measurement matrix is ready, we can apply the PCAMD algorithm to compute the complete set of mesh nodes and transformations among different views. The object model is then obtained based on the known connectivity among all mesh nodes.
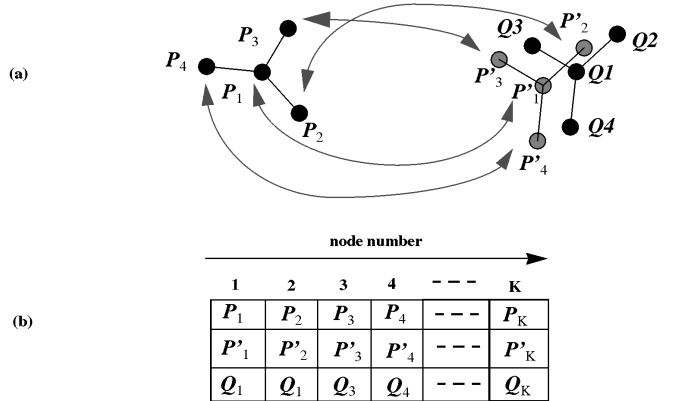

Fig. 3. One-to-one matching: (a) valid correspondence between nodes; (b) table of correspondences.

4 How to Integrate: Principal Component Analysis with Missing Data

4.1 Multiple View Merging

Our task is to model a free-form object from a sequence of range images. Suppose that the model consisting of 20 nodes is observed from four views. If the correspondence among 20 mesh nodes over four views is obtained, we can form a 16×20 measurement matrix

$$\mathbf{W} = \begin{bmatrix} \mathbf{P}_1^{(1)} & \mathbf{P}_2^{(1)} & \mathbf{P}_3^{(1)} & \mathbf{P}_4^{(1)} & \cdots & \mathbf{P}_{14}^{(1)} & \mathbf{P}_{15}^{(1)} & * & \cdots & * \\ \mathbf{P}_1^{(2)} & \mathbf{P}_2^{(2)} & \mathbf{P}_3^{(2)} & \mathbf{P}_4^{(2)} & \cdots & * & \mathbf{P}_{15}^{(2)} & \mathbf{P}_{16}^{(2)} & \cdots & * \\ \mathbf{P}_1^{(3)} & \mathbf{P}_2^{(3)} & * & * & \cdots & \mathbf{P}_{14}^{(3)} & * & \mathbf{P}_{16}^{(3)} & \cdots & * \\ * & * & * & * & \cdots & * & \mathbf{P}_{15}^{(4)} & \mathbf{P}_{16}^{(4)} & \cdots & \mathbf{P}_{20}^{(4)} \end{bmatrix}, \quad (4)$$

where $\mathbf{p}_p^{(f)} = \left(x_p^{(f)}, y_p^{(f)}, z_p^{(f)}, 1 \right)^T$, $f = 1, ..., 4$, $p = 1, ..., 20$ represents homogeneous coordinates of vertex p at frame f, and every * indicates an unobservable node. The task now is to recover the positions of all 20 points in a fixed coordinate system.

If the measurement matrix were complete, our task would be to average all those 20 points over four views, assuming that the input data is noisy. The standard way to solve this problem is to apply the singular value decomposition (SVD) to the matrix W, whose rank is, at most, four. The measurement matrix can subsequently be factorized, with proper normalization, into a left matrix Q of transformation parameters and a right matrix $\mathbf{P}$ of homogeneous coordinates $\mathbf{W} = \mathbf{QP}$, where

$$\mathbf{Q} = \begin{bmatrix} Q^{(1)^T} & Q^{(2)^T} & Q^{(3)^T} & Q^{(4)^T} \end{bmatrix}^T, \quad P = \begin{bmatrix} \mathbf{p}_1 & \mathbf{p}_2 & \cdots & \mathbf{p}_{20} \end{bmatrix}, \quad (5)$$

$Q^{(f)}$ is the transformation of fth view with respect to the fixed world coordinate system, and $\mathbf{p}_p$ is the pth vertex in the same world coordinate system.

In practice, the measurement matrix is often incomplete; it is not unusual for a large portion of the matrix to be unobservable.

When the percentage of missing data is very small, it is possible to replace the missing elements by the mean or by an extreme value; this is a useful strategy in multivariate statistics. However, such an approach is no longer valid when a significant portion of the measurement matrix is unknown.

Therefore, object modeling from a sequence of views should be formulated as a problem of PCAMD, which has been studied in computational statistics [14], [22]. We have modified Wiberg's formulation [22] of principal component analysis with missing data, and generalized the problem as a weighted least square (WLS) problem [15].

4.2 Two-Step WLS Problem

We now apply the PCAMD algorithm to the following free-form object modeling problem. Suppose that we have correspondence of P mesh nodes over F frames. In the case of global resampling, the number of mesh nodes is known and fixed. We then have trajectories of point coordinates $\mathbf{v}_p^{(f)}$ for $f = 1, ..., F$ and $p = 1, ..., P$, where $\mathbf{v}_p^{(f)}$ is the pth point in the fth frame. Instead of forming a $4F \times P$ measurement matrix, as in Section 4.1, we assemble registered measurement matrices $\mathbf{W}^{(v)}$ and $\mathbf{W}^{(d)}$ from the original measurement $3F \times P$ matrix $\mathbf{W}$ formed from trajectories of $\mathbf{v}_{fp}$ in the same way as in (4). After removing the translation component, we get

$$\mathbf{W}^{(v)} = \mathbf{W} - \mathbf{t}\mathbf{M}, \qquad (6)$$

where $\mathbf{M}$ is a row vector of all ones, and $\mathbf{t}$ is a column vector consisting of the translation vector of each view with respect to the world coordinate system, i.e.,

$$\mathbf{M} = \begin{bmatrix} [1 & 1 & 1] \dots [1 & 1 & 1] \end{bmatrix}, \quad \mathbf{t} = \begin{bmatrix} \begin{bmatrix} t_{1x} & t_{1y} & t_{1z} \end{bmatrix}^T \\ \dots \\ \begin{bmatrix} t_{px} & t_{py} & t_{pz} \end{bmatrix}^T \end{bmatrix}. \qquad (7)$$

Similarly, after removing the rotation component, we have

$$\mathbf{W}^{(d)} = \mathbf{W} - \mathbf{R}\mathbf{V}, \qquad (8)$$

where $\mathbf{R}$ is the rotation matrix of each view with respect to the world coordinate system, and $\mathbf{V}$ is the point matrix in the world coordinate system, i.e.,

$$\mathbf{V} = \begin{bmatrix} \mathbf{v}_1 & \dots & \mathbf{v}_p \end{bmatrix}, \quad \mathbf{R} = \begin{bmatrix} R^{(1)} \\ \dots \\ R^{(F)} \end{bmatrix}. \qquad (9)$$

Initially $\mathbf{R}$ and $\mathbf{t}$ can be obtained using mesh matching technique described in Section 3.2.

It can be easily shown that $\mathbf{W}^{(v)}$ has, at most, rank three and $\mathbf{W}^{(d)}$ has rank one when noise-free; therefore, $\mathbf{W}^{(v)}$ and $\mathbf{W}^{(d)}$ are highly rank-deficient. We decompose $\mathbf{W}^{(v)}$ into

$$\mathbf{W}^{(v)} = \mathbf{R}\ \mathbf{V}. \qquad (10)$$

Similarly, we can decompose $\mathbf{W}^{(d)}$ into

$$\mathbf{W}^{(d)} = \mathbf{t}\ \mathbf{M}. \qquad (11)$$

When all elements in the two measurement matrices are known, we need to solve two least-squares problems. However, since only part of the object is visible in each view, we end up with two WLS problems instead. The first least squares problem, labeled as WLS-R, is

$$\min \sum_{f=1,...,F,\ p=1,...,P} \left(\gamma_{f,p} \left(\mathbf{W}_{f,p}^{(v)} - \left[\mathbf{R}\mathbf{V} \right]_{f,p} \right) \right)^2 \qquad (12)$$

and the second one, denoted as WLS-T, is

$$\min \sum_{f=1,...,F,\ p=1,...,P} \left(\gamma_{f,p} \left(\mathbf{W}_{f,p}^{(d)} - \left[\mathbf{t}\mathbf{M} \right]_{f,p} \right) \right)^2 \qquad (13)$$

where $\gamma_{f,p} = 0$ if the point p is invisible in frame f, and $\gamma_{f,p} = 1$ otherwise. All weights can be between zero and one, depending on the confidence of each measurement.

4.3 Iterative Algorithm

We have devised a two-step algorithm which solves the WLS-R and, subsequently, the WLS-T by applying the PCAMD algorithm to both problems. The WLS-R problem has been decomposed into F minimization problems and solved by employing the quaternion representation of rotation in the same way as in [15]. The two-step algorithm is as follows:

Algorithm two-step WLSs

Step 0 Initialization

> **(0.1) read in measurement matrices**
> **(0.2) read in weight matrices γ**

Step 1 WLS-R

> **(1.1) register $\mathbf{W}^{(v)}$ from W and t**
> **(1.2) apply PCAMD to update R and V**
> **(1.3) go to (1.2) if not converged; otherwise, advance to Step 2**

Step 2 WLS-T

> **(2.1) register $\mathbf{W}^{(d)}$ from W, R, and V**
> **(2.2) apply PCAMD to update the translation t**
> **(2.3) stop if converged; otherwise go to step 1.**

Because the measurement matrix is rank-deficient, there are infinite solutions to the minimization problem unless an additional constraint is imposed. In our implementation, we normalize the decomposition by aligning the first coordinate with the world coordinate system, i.e., the first rotation matrix is identity and the first translation is zero.

5 EXPERIMENTS

In this section, we present the results of applying our algorithm to real range image sequences of a free-form object. The reader is referred to [16] for more real object examples and demonstration of robustness of our approach using synthetic data.

The range images used in our experiments were taken using a light-stripe range finder which has a resolution of 0.2 mm. The objects were placed on a rotary table about one meter in front of the range finder. To obtain the ground truth of the transformation, rotation axis and rotation center of the rotary table are calibrated using a known geometry calibration cube (see Appendix of [16]). Fig. 4 shows deformable surfaces of four different views. The occluded part of the object is interpolated in the deformable surface mesh of each view. The reconstructed object models in different resolutions are shown in Fig. 5.

To compare the result of the PCAMD algorithm with that of the sequential method, we show the reconstruction errors at each mesh node in Fig. 6, where the mean error and maximum error for the integral method are 2.7 and 9.2, as opposed to 3.7 and 16.8 for the sequential method. The error at each mesh node of the reconstructed model (sequential or integral) is defined as the minimum distance between this node and the original shape. Other examples of errors at the cross-section contours of reconstructed models (with 980 mesh nodes) can also be found in [16].

6 CONCLUDING REMARKS

An integral approach to free-form object modeling using multiple range images has been described in this paper. To reconstruct free-form object models from often incomplete and noisy range images, our approach successfully integrates multiple views by addressing
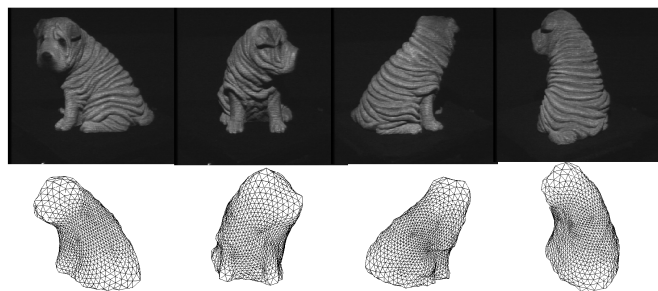
Fig. 4. Examples of deformable models from different views.
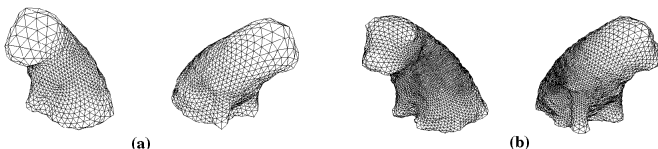

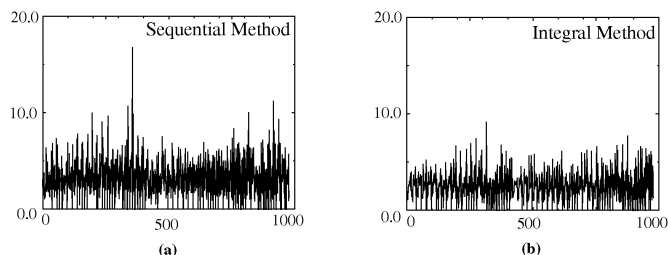Fig. 5. Reconstructed models: (a) lower resolution: 980 nodes, (b) higher resolution: 3,380 nodes.

Fig. 6. Comparison between PCAMD and Sequential methods: error at each mesh node (total number is 980). (a) sequential method; (b) PCAMD.

two questions: what to integrate and how to integrate. One significant contribution of this work is that statistically optimal free-form object models are recovered by applying the algorithm of principal component analysis with missing data (PCAMD).

Another contribution of this work is the global resampling scheme, which solves the problem of what to integrate. Global resampling is achieved using salient feature points which reliably encode local curvature information by taking local connectivity into account. Because of the global resampling, spatial connectivity among different mesh nodes is easily established, leading to the simple construction of object models. Experiments indicate that our approach converges quickly and produces good models, even in the presence of noise. An accurate free-form object model reconstructed from a sequence of real range images is presented.

One drawback of global resampling is its trade-off of accuracy vs. robustness. To obtain more accurate object models, we can use a coarse-to-fine global resampling scheme. The object models at different levels of detail can then be represented. A simple coarse-to-fine pyramid can be implemented using tessellation at different levels. Another way of building more accurate models is to use adaptive surface subdivision on the coarse level model. Real range data can be filtered by coarse level models before the process of adaptive subdivision.

An alternative to global resampling is local resampling. Local resampling uses sample data points in the local object space (i.e., directly from the range image) and establishes correspondence among different views (e.g., using the ICP algorithm [3]). Statistically optimal object models are obtained by applying the same algorithm developed for global resampling in this paper, provided that the connectivity among all sample points can be established [19].

The global resampling scheme can be used to develop an efficient three-dimensional object shape similarity metric because of the one-to-one correspondence between two meshes. This distance between two spherical representations can also be used to derive an active sampling method, such that a minimum number of views is required to construct a complete model.

REFERENCES

[1] N. Ahuja and J. Veenstra, "Generating Octrees from Object Silhouettes in Orthographic Views," *IEEE Trans. Pattern Analysis and Machine Intelligence*, vol. 11, no. 2, pp. 137-149, Feb. 1989.
[2] F. Arman and J.K. Aggarwal, "Model-Based Object Recognition in Dense-Range Images—A Review," *ACM Computing Surveys*, vol. 25, no. 1, pp. 5-43, 1993.
[3] P. Besl and N.D. Kay, "A Method for Registration of 3-D Shapes," *IEEE Trans. Pattern Analysis and Machine Intelligence*, vol. 14, no. 2, pp. 239-256, Feb. 1992.
[4] B. Bhanu, "Representation and Shape Matching of 3-D Objects," *IEEE Trans. Pattern Analysis and Machine Intelligence*, vol. 6, pp. 340-351, 1984.
[5] G. Champleboux, S. Lavallee, R. Szeliski, and L. Brunie, "From Accurate Range Imaging Sensor Calibration to Accurate Model-Based 3-D Object Localization," *Proc. IEEE Computer Vision and Pattern Recognition Conf.*, pp. 83-89, June 1992.
[6] Y. Chen and G. Medioni, "Object Modeling by Registration of Multiple Range Images," *Proc. IEEE Int'l Conf. Research and Applications*, pp. 2,724-2,729, Apr. 1991.
[7] Y. Chen and G. Medioni, "Surface Description of Complex Objects from Multiple Range Images," *Proc. IEEE Computer Vision and Pattern Recognition Conf.*, pp. 153-158, June 1994.
[8] H. Delingette, M. Hebert, and K. Ikeuchi, "A Spherical Representation for the Recognition of Curved Objects," *Proc. Int'l Conf. Computer Vision '93*, Berlin, 1993.
[9] F.P. Ferrie and M.D. Levine, "Integrating Information from Multiple Views," *Proc. IEEE Workshop Computer Vision*, pp. 117-122, 1987.
[10] K. Higuchi, M. Hebert, and K. Ikeuchi, "Building 3-D Models from Unregistered Range Images," *CVGIP-GMIP*, vol. 57, no. 4, pp. 315-333, July 1995.
[11] H. Hoppe, T. DeRose, T. Duchamp, M. Halstead, H. Jin, J. McDonald, J. Schweitzer, and W. Stuetzle, "Piecewise Smooth Surface Reconstruction," *Computer Graphics SIGGRAPH '94*, pp. 295-302, 1994.
[12] T. McInerney and D. Terzopoulos, "A Finite Element Model for 3D Shape Reconstruction and Nonrigid Motion Tracking," *Proc. Fourth Int'l Conf. Computer Vision*, pp. 518-523, 1993.
[13] B. Parvin and G. Medioni, "B-Rep from Unregistered Multiple Range Images," *Proc. IEEE Int'l Conf. Research and Applications*, pp. 1,602-1,607, May 1992.
[14] A. Ruhe, "Numerical Computation of Principal Components When Several Observations Are Missing," Technical Report UMINF-48-74, Dept. of Information Processing, Umea Univ., Umea, Sweden, 1974.
[15] H. Shum, K. Ikeuchi, and R. Reddy, "Principal Component Analysis with Missing Data and Its Application to Object Modeling," *IEEE Trans. Pattern Analysis and Machine Intelligence*, vol. 17, no. 9, pp. 854-867, Sept. 1995.
[16] H. Shum, M. Hebert, K. Ikeuchi, and R. Reddy, "An Integral Approach to Free-Form Object Modeling," Technical Report CMU-CS-95-135, Carnegie Mellon Univ., May 1995.
[17] M. Soucy and D. Laurendeau, "Multi-Resolution Surface Modeling from Multiple Range Views," *Proc. IEEE Computer Vision and Pattern Recognition Conf. '92*, pp. 348-353, 1992.
[18] G. Taubin, "Estimating the Tensor of Curvature of a Surface from a Polyhedral Approximation," *Proc. Int'l Conf. Computer Vision '95*, pp. 902-907, 1995.
[19] G. Turk and M. Levoy, "Zippered Polygon Meshes from Range Images," *Computer Graphics SIGGRAPH '94*, pp. 311-318, 1994.
[20] M. Vasilescu and D. Terzopoulos, "Adaptive Meshes and Shells," *Proc. IEEE Computer Vision and Pattern Recognition Conf. '92*, pp. 829-832, 1992.
[21] B.C. Vemuri and J.K. Aggarwal, "3-D Model Construction from Multiple Views Using Range and Intensity Data," *Proc. Computer Vision and Pattern Recognition Conf.*, pp. 435-437, 1986.
[22] T. Wiberg, "Computation of Principal Components When Data Are Missing," *Proc. Second Symp. Computational Statistics*, pp. 229-236, Berlin, 1976.